NASA / CR—2000-210460

Suppression of Cavity-Driven Flow Separation in a Simulated Mixed Compression Inlet

Bruce J. Wendt
Modern Technologies Corporation, Middleburg Heights, Ohio

September 2000

The NASA STI Program Office . . . in Profile

Since its founding, NASA has been dedicated to the advancement of aeronautics and space science. The NASA Scientific and Technical Information (STI) Program Office plays a key part in helping NASA maintain this important role.

The NASA STI Program Office is operated by Langley Research Center, the Lead Center for NASA's scientific and technical information. The NASA STI Program Office provides access to the NASA STI Database, the largest collection of aeronautical and space science STI in the world. The Program Office is also NASA's institutional mechanism for disseminating the results of its research and development activities. These results are published by NASA in the NASA STI Report Series, which includes the following report types:

- TECHNICAL PUBLICATION. Reports of completed research or a major significant phase of research that present the results of NASA programs and include extensive data or theoretical analysis. Includes compilations of significant scientific and technical data and information deemed to be of continuing reference value. NASA's counterpart of peer-reviewed formal professional papers but has less stringent limitations on manuscript length and extent of graphic presentations.

- TECHNICAL MEMORANDUM. Scientific and technical findings that are preliminary or of specialized interest, e.g., quick release reports, working papers, and bibliographies that contain minimal annotation. Does not contain extensive analysis.

- CONTRACTOR REPORT. Scientific and technical findings by NASA-sponsored contractors and grantees.

- CONFERENCE PUBLICATION. Collected papers from scientific and technical conferences, symposia, seminars, or other meetings sponsored or cosponsored by NASA.

- SPECIAL PUBLICATION. Scientific, technical, or historical information from NASA programs, projects, and missions, often concerned with subjects having substantial public interest.

- TECHNICAL TRANSLATION. English-language translations of foreign scientific and technical material pertinent to NASA's mission.

Specialized services that complement the STI Program Office's diverse offerings include creating custom thesauri, building customized data bases, organizing and publishing research results . . . even providing videos.

For more information about the NASA STI Program Office, see the following:

- Access the NASA STI Program Home Page at ***http://www.sti.nasa.gov***

- E-mail your question via the Internet to help@sti.nasa.gov

- Fax your question to the NASA Access Help Desk at (301) 621-0134

- Telephone the NASA Access Help Desk at (301) 621-0390

- Write to:
  NASA Access Help Desk
  NASA Center for AeroSpace Information
  7121 Standard Drive
  Hanover, MD 21076

NASA / CR—2000-210460

Suppression of Cavity-Driven Flow Separation in a Simulated Mixed Compression Inlet

Bruce J. Wendt
Modern Technologies Corporation, Middleburg Heights, Ohio

Prepared under Contract NAS3–99138

National Aeronautics and
Space Administration

Glenn Research Center

September 2000

Acknowledgments

When a project spans the duration of 5 years, it may be impossible to credit all of the essential players. However, a few names stick out. The author would like to thank Warren Hingst (now retired from NASA Glenn) and Bobby Sanders (of Techland) for overall design guidance and early program advocacy. Craig McArthur (now at NASA Marshall) provided essential operating guidance. Jennifer Kolden (of Boeing Aircraft Company) provided the subsonic diffuser designs and many insights into performance features. Dave Saunders (of NASA Glenn) contributed with his knowledge and his discussions of supersonic inlet design and function. Supporting facility design efforts were effectively conducted by Ron Romanchok (NASA Glenn), John Gallagher (also of NASA Glenn), and Bernie Drapp (ADF). Phil Blumenthal (of Dynacs Engineering) was responsible for the instrumentation of the many complex hydraulic/electronic control systems required for the operation of this test. Winston Johnson provided mechanical and operational support. The last leg of this project, and this report, could not have been possible without the funding provided by NASA Glenn's Propulsion Systems Base Program and the Supersonic Propulsion Technology Project headed by Mary Jo Long-Davis. Finally, special thanks to the boys of Rancid whose loud and cryptic words helped me through many a long night.

Available from

NASA Center for Aerospace Information
7121 Standard Drive
Hanover, MD 21076
Price Code: A03

National Technical Information Service
5285 Port Royal Road
Springfield, VA 22100
Price Code: A03

Available electronically at http://gltrs.grc.nasa.gov/GLTRS

SUPPRESSION OF CAVITY-DRIVEN FLOW SEPARATION IN A SIMULATED MIXED COMPRESSION INLET

B.J. Wendt*
Modern Technologies Corporation
Middleburg Heights, Ohio 44130

Abstract

A test facility designed to simulate a bifurcated subsonic diffuser operating within a mixed compression inlet is described. The subsonic diffuser in this facility modeled a bypass cavity feature often used in mixed compression inlets for engine flow matching and normal shock control. A bypass cavity-driven flow separation was seen to occur in the subsonic diffuser without applied flow control. Flow control in the form of vortex generators and/or a partitioned bypass cavity cover plate were used to eliminate this flow separation, providing a 2% increase in area-averaged total pressure recovery, and a 70% reduction in circumferential distortion intensity.

Introduction and Background

The time constraints of an ever-shrinking world are the fundamental driving forces behind recent efforts to expand supersonic cruise flight capability for passenger aircraft. The High Speed Research (HSR) Program, a partnership between the U. S. aerospace industry and NASA, was charged with developing the technology to enable the manufacture and operation of a fleet of quiet, efficient, and environmentally sound supersonic commercial transports. These large 300-passenger aircraft were to be known as "High Speed Civil Transports" or HSCTs. The HSR program was terminated in the fall of 1999, due to a perceived lack of interest in the world aviation market for HSCTs.

The HSCT propulsion system configuration, at the point of program termination, is diagrammed in Figure 1a. The system consisted of a mixed flow turbofan, a two-dimensional mixed compression bifurcated inlet, and a two-dimensional convergent-divergent mixer-ejector nozzle. For purposes of clarity, the inlet and nozzle are drawn 90° out of their proper rotational alignment. Cruise conditions were to occur at 60,000 feet with an external Mach number of about 2.4. The entire system was rated for about 55,000 lbf of thrust. The mechanically complex and seemingly oversized nozzle was deemed necessary to meet stringent noise and emission standards projected for the supposed time of first flight.

The massive nozzle made it imperative to reduce the weight of the other components in the propulsion cycle. Partially in response to this concern, the bifurcated inlet design was chosen. The term "bifurcated" is used because the inlet splits the captured mass flow intended for one turbofan and initially divides it into two equal streams. The advantage of such an arrangement over a two-dimensional single-stream inlet (both the Russian Tu-144 and the Concorde are single-stream types) is one of potential length (and thereby weight) reduction. A supersonic diffuser in a bifurcated design is conceptually 50% shorter than a corresponding single-stream inlet duct designed for the same captured mass flow.[1] The HSCT propulsion system also would require large mass flows at transonic conditions. The two-dimensional bifurcated inlet, with its collapsible centerbody (or "ramp"), was ideally suited for supplying these mass flows at transonic conditions.

Figure 1b is an expanded sketch of the bifurcated mixed-compression inlet. A combination of oblique shocks and internal compression comprise the upstream supersonic diffuser. This region of the inlet terminates in a normal shock nominally located at the throat or upstream end of the subsonic diffuser. An elaborate bleed system is used to control the boundary layer and shock impingement locations in the supersonic diffuser. A region of bleed at the throat location, and a bypass bleed system (located at the aft end of the subsonic diffuser), are used to ensure normal shock stability and control in the diffuser throat. Cross-sectional area expansion and vortex generators are used to provide for (and to control) further compression in the subsonic diffuser region. Heavy lines are used in Figure 1b to emphasize the flow surfaces of the subsonic diffuser. This type of diffuser is referred to as a "bifurcated transitioning S-diffuser" due to the cross-sectional area change (from dual-rectangular to semiannular) and a slight S-shaped centerline curvature. Figure 1b also includes an oblique view of the main surface features of the subsonic diffuser, indicating the locations of throat, sidewalls, ramp, cowl, bypass cavity, and engine face plane. The length-to-diameter or "L/D" ratio, and the cross-sectional area ratio, A_e/A_t, characterize the overall geometry of this type of subsonic diffuser. In these expressions L is the axial distance between throat and engine face planes, D is the engine face diameter, and (A_t, A_e) are the cross-sectional areas of throat and circular engine face, respectively.

*Resident Research Engineer at NASA Glenn Research Center, Inlet Branch.

The bypass cavity is a safety and control feature typically included in the design of the mixed compression inlet. The bypass cavity performs the following primary functions:

1. In the extreme event that an engine rotor should lock-up during operation, a set of large valves located downstream in the bypass cavity open. The entire airflow meant for the engine is thus rerouted through the bypass cavity channel.
2. Should the engine undergo a sudden transient in its operational condition (such as a surge or a stall) the bypass cavity valves open to reroute a portion of the air meant for the engine. This is done with the aim of preventing the inlet shock train from jumping out in front of the inlet or "unstarting". Air routed through the bypass cavity is also used to match engine airflow requirements under more typical operations (aircraft maneuvers and throttle commands for both on and off-design conditions).
3. A small amount of air or "trim" flow is routed through the bypass cavity (using a set of smaller valves) to position the normal shock near the inlet throat and/or to provide some flow for engine cooling.

The bypass cavity is sized to accommodate the locked rotor case. To minimize its impact on the performance of the inlet, the bypass cavity is placed at the tail end of the subsonic diffuser where the cross-sectional area expansion has vanished. Even with this precaution, however, the inclusion of the bypass cavity into the design of the subsonic diffuser often comes with a price. This penalty is a degradation of the airstream entering the engine compressor at cruise conditions. Figure 2 illustrates the engine face Pitot pressure profile of a bifurcated mixed compression inlet operating at cruise in a free stream with Mach number 2.7.[2] The subsonic diffuser for this inlet had an L/D = 3.2 and a cross-sectional area ratio = 1.6. The horizontal line running through the center of the annular engine face represents the trailing edge of the upstream ramp. The two low momentum "lumps" of fluid at the 12 and 6 o'clock positions result (in major part) from a flow separation driven by the bypass cavity. To see that this is so, consider Figure 3. Figure 3 illustrates the engine face Pitot pressure contours downstream of a bifurcated subsonic diffuser with L/D = 2.7 and cross-sectional area ratio = 1.6. The inflow or throat Mach number is 0.79 (identical to the case illustrated in Figure 2). The experimental grid resolution in Figure 3 is much higher than that used in Figure 2, but the results show essentially the same features: a lump of low momentum fluid on the cowl surfaces at the 12 and 6 o'clock positions. Surface oil flow visualization conducted at the aft end of this subsonic diffuser reveals the pattern illustrated in Figure 4. A pair of vortices is evident on the downstream-facing side of the bypass cavity at the top and bottom positions. These vortices entrain fluid from the bypass cavity and spill it into the core stream, thereby creating the low-momentum fluid regions observed in the Pitot pressure profiles at the engine face plane. The primary objective of this paper is to describe the results of two flow control techniques used to suppress this vortical-driven flow separation. The bifurcated subsonic diffuser used in this study had L/D = 2.3 and a cross-sectional area ratio of 1.9. Qualitative results in the form of surface oil flow traces are presented. Quantitative results are also presented. These include Pitot pressure contours (low and high grid resolution) at the engine face, and the derived performance descriptors of area-averaged total pressure recovery and circumferential distortion intensity. This paper will also describe and illustrate a unique facility designed and fabricated to test bifurcated subsonic diffusers for mixed compression inlets.

Test Facilities

Experiments conducted on bifurcated subsonic diffusers designed for the HSR propulsion system were carried out at NASA Glenn's Internal Fluid Mechanics Facility located in test cell W1B. The subsonic diffusers were modeled in precise geometry from the throat cross-section to the engine face plane (hereafter referred to as the "Aerodynamic Interface Plane" or "AIP"). Figure 5 illustrates the entire test section used in the effort to mimic a bifurcated subsonic diffuser within a mixed compression inlet.

Dry air pressurized to 1 atmosphere entered a contraction nozzle at the upstream end of the test section. The contraction nozzle split the airstream into two equal portions, each portion routed to a rectangular inflow channel. Each inflow channel was equipped with a pair of convergent-divergent (CD) nozzle-plates. These plates induced the airstream to expand supersonically to a Mach number of 1.3 (the facility could also be operated with subsonic inflow by changing out the CD plates for flat plates).

The diffuser throat was located at the downstream end of the rectangular inflow channels. At the throat location the airstream shocked down in what was nominally a normal shock. A band of perforated surface provided a stabilizing bleed for this shock. The bleed band extended around the full perimeter of each rectangular channel and had a potential axial length of 0.6D. The shading in Figure 5 indicates the bleed band. The bleed surface consisted of normal holes in a staggered pattern having 42% porosity (open area). These holes were 1/8" in diameter and were drilled into a surface plate with a thickness of 1/8". The boundary

layer blockage in the throat was about 2.5% based on the measured boundary layer displacement thickness there. To obtain inflow conditions representative of those in the throat of a mixed compression inlet, it was necessary to limit the axial extent of the bleed region to about 0.35D. The unchoked bleed on each surface (cowl, ramp, or sidewalls) could be independently controlled through the use of choked bleed plugs located downstream in each of six lines. Figure 6 is a cross-section of the throat illustrating the arrangement of throat bleed surfaces, bleed plenums, and bleed lines. Bleed flows through each line were adjusted to ensure that the bleed rate per surface area was the same on all surfaces.

As mentioned earlier, the subsonic diffuser studied in this test had L/D = 2.3 and an area ratio = 1.9. The diffuser geometry was further constrained such that the throat width was equal to the AIP diameter D. This held over the full axial length of the diffuser and was also a characteristic of the entire test section (to the exhaust pipe). Engineers at the Boeing Aircraft Company designed the internal lines of the diffuser. The bypass cavity feature included a set of fixed circumferential louvers. The cavity could be bled at a rate equal to about 2% of the total flow through the test section.

Upon exiting the diffuser, the recombined airstream flowed through an instrumentation duct, a contraction section, and entered the (vacuum) altitude exhaust line.

Figure 7 diagrams the overall facility and highlights its main operational features. The pressurized source air was routed through a flow conditioning plenum and a round-to-rectangular bellmouth before it entered the test section. The plenum contained a honeycomb and various screens to reduce the turbulence intensity in the source air supplied to the test section. The diffuser was backpressured by a plug valve located in the altitude exhaust line. Both the test section and the bleed manifold plenum dumped air into the altitude exhaust line. The near-vacuum condition in the altitude exhaust line was maintained by NASA Glenn's centrally located compressor system. The flow rate through the test section was typically about 18 lbm/sec. The flow rate through the bleed system and manifold plenum was typically about 1 lbm/sec.

Flow conditions in the test section and diffuser were monitored and recorded using axial rows of surface static pressure taps. The locations of these taps are indicated in Figure 5. The Pitot pressure field in the AIP was recorded using a pair of 3-tip rakes (also illustrated in Figure 5). These rakes were actuated in both the radial and circumferential components of the AIP with nearly unlimited resolution possible. All pressure data was recorded for this test using the Electro-Scan Pressure (ESP) System. The periodically calibrated ESP System measured the absolute value of pressure (in units of psia) to within ±0.003 psid.

Figure 8 illustrates the flow control apparatus used in this study. A spanwise row of mounting holes for vortex generators was located a little downstream of the diffuser throat. These mounting holes were spaced roughly 0.6 inches apart and extended about the full perimeter of the diffuser (in both flow channels). In the absence of vortex generators these mounting holes were filled with cylindrical plugs. The vortex generators were blade-type devices having a cross-sectional profile equivalent to a NACA 0012 split down the line of symmetry. These vortex generators came in the two sizes illustrated in Figure 8. In addition to the vortex generators, the bypass cavity louvers were machined to accept a cover plate which blocked off the bypass cavity at two locations. Figure 8 indicates the manner in which this bypass cover plate partitioned the bypass cavity. The bypass cover plate was designed to block the recirculating flows observed in previous studies (refer to Figures 3 and 4) without significantly impairing the shock-stabilizing function of the bypass cavity.

Results

Diffuser Performance Descriptor Definition

The diffuser performance descriptors evaluated in this study are area-averaged total pressure recovery and total pressure distortion intensity. These descriptors are determined for two types of cross-plane survey grids acquired at the engine face by the facility's two Pitot probe rakes. Figure 9 illustrates these two survey grids.

On the left in Figure 9 is the low-resolution grid constructed to mimic standard 40-probe engine face rake geometry. This grid was used to obtain cross-plane surveys of engine face Pitot pressure profiles in a time-efficient manner. Refer to Figure 9 and the following discussion for an explanation of its construction. First, we divide the circular area (defined by the cowl flow surface) into eight identical pie-shapes. Second, we divide the annular engine face into five doughnut-shapes of equal area. At the centroid of each sub-area, formed by the intersecting boundaries of the pie and doughnut-shapes, place a grid point. Note from Figure 9 how the grid was oriented relative to the trailing edge of the diffuser ramp.

The high-resolution grid is illustrated on the right hand side of Figure 9. The high-resolution grid was used for detailed surveys of Pitot pressure at the engine face plane. In the high-resolution grid, $\Delta\theta = 10°$ and $\Delta r = 0.2$ inches. The total number of grid points was 684.

An area-average of a quantity β over an annular section of angular extent $\Delta\theta = b - a$ and radial extent $\Delta r = d - c$ is defined as:

$$\overline{\beta}(a,b:c,d) = \frac{\int_a^b \int_c^d \beta r \, dr \, d\theta}{\int_a^b \int_c^d r \, dr \, d\theta}. \quad (1)$$

Define P to be the nondimensional pressure obtained by dividing the total pressure, measured at any point in the cross-plane, by the reference total pressure, or:

$$P \equiv p_t / p_{tref}. \quad (2)$$

Area-averaged total pressure recovery, or AATPR, is defined from Equation (1) by letting $\beta = P$, $a = 0$, $b = 2\pi$, $c = r_o$ (hub radius), and $d = R$ (AIP radius). Thus we can write:

$$AATPR = \overline{P}(0,2\pi : r_o, R). \quad (3)$$

In a similar fashion, the circumferential distortion intensity DC60 is defined as:

$$DC60 = \frac{\overline{p}_t(0,2\pi : r_o, R) - \overline{p}_t(\theta,\theta+\Delta\theta : r_o, R)_{\min}}{\overline{q}(0,2\pi : r_o, R)} \quad (4)$$

where $\Delta\theta = \pi/3$, $\overline{p}_t(\theta,\theta+\Delta\theta : r_o, R)_{\min}$ is the minimum value of $\overline{p}_t(\theta,\theta+\Delta\theta : r_o, R)$ occurring over the entire annular cross-plane, and q is the dynamic pressure.

The radial profile of circumferential distortion intensity, termed "sixty degree ring sector distortion" or 60DRSD is defined for a ring of radius r_i and thickness Δr:

$$60DRSD = \frac{\overline{p}_t(a,b:c,d) - \overline{p}_t(\theta,\theta+\Delta\theta : c,d)_{\min}}{\overline{p}_t(a,b:c,d)} \quad (5)$$

where $a = 0$, $b = 2\pi$, $c = r_i - \Delta r/2$, $d = r_i + \Delta r/2$, $\Delta\theta = \pi/3$, and $\overline{p}_t(\theta,\theta+\Delta\theta : c,d)_{\min}$ is the minimum value of $\overline{p}_t(\theta,\theta+\Delta\theta : c,d)$ occurring over the full circular ring. As an example, the high-resolution grid illustrated in Figure 9 is naturally divided into 19 such rings.

A general description of the distortion intensity is provided by the so-called "DH" factor defined as:

$$DH = \frac{p_{t\max} - p_{t\min}}{\overline{p}_t(0,2\pi : r_o, R)}. \quad (6)$$

In Equation (6) p_{tmax} and p_{tmin} are the maximum and minimum values of total pressure acquired over the cross-plane grid.

Diffuser Test Operational Procedure

Let us now review a typical diffuser performance test sequence to establish the connection between flow phenomena occurring in the throat of the diffuser and the performance recorded downstream at the engine face plane. Figure 10 illustrates the diffuser throat geometry and terminal shock locations as the subsonic diffuser is back-pressured from its initial "super-critical" condition (state 1) to its final "sub-critical" condition (state 6). At each of the six terminal shock locations illustrated in Figure 10 a profile of the streamwise surface static pressure ratio was acquired (left hand side of Figure 10) and a profile of the Pitot pressure was obtained at the engine face plane (right hand side of Figure 10). The surface static pressure ratio identified local flow conditions through the inflow channels and diffuser model as well as aided in identifying terminal shock position. The Pitot pressure profile at the engine face established diffuser performance in terms of AATPR and the various distortion descriptors. The Pitot pressure contours illustrated in Figure 10 are based on the low-resolution survey grid. At the critical point (state 4) both low and high-resolution surveys were typically acquired. AATPR derived from data acquired on the low-resolution grid is denoted AATPR40. AATPR40 and throat bleed mass flow data are combined to create "cane recovery curves" such as that illustrated in the lower middle portion of Figure 10. Each point on the cane recovery curve corresponds to one of the six states (or terminal shock locations):

1. State 1 is the super-critical state. State 1 was obtained by applying the minimum backpressure condition to the diffuser model. In state 1 the terminal shock was approximately 0.60D into the diffuser. The cross-sectional area here was slightly larger than the throat area and the local flow had expanded to a Mach number condition greater than 1.3. The flow shocked down here with the largest drop in recovery as indicated in Figure 10. The throat bleed was adjusted to its desired test level when the diffuser was in the supercritical state. In the case of the cane curve plotted in Figure 10 the total amount of throat bleed mass flow was 5% of the flow through the diffuser. The overall bleed condition in the throat was known as a "fixed-bleed exit" condition. This term refers to the fact that the backpressure condition for the bleed remained constant. Thus, as long as the throat bleed region remained at the minimum static pressure (i.e. with the terminal shock located downstream), the bleed rate remained unchanged.
2. When the main duct backpressure was raised a bit, the terminal shock moved upstream towards the throat by about 0.20D. This condition was known as the intermediate state 2. The cross-sectional area of the duct had decreased somewhat here and so the terminal

shock was weaker. As a result, the static pressure rose in the downstream portion of the diffuser. Total pressure recovery at the engine face plane rose correspondingly.

3. The backpressure was raised again until the shock sat at the downstream end of the porous bleed band encompassing the throat. A further decrease in cross-sectional area between states 2 and 3 was responsible for reducing the shock strength further resulting in an additional rise in static and total pressure recovery at the engine face plane.
4. As the terminal shock moved across the bleed band towards the geometric throat plane, the cross-sectional area change became negligible. However, the static and total pressure recoveries continued to climb. This occurred because, as the throat bleed band became pressurized due to the presence of the shock, the bleed rates started to climb. As the bleed rates climbed the inflow boundary layers thinned and a portion of the duct core flow was angled towards the wall. These effects increased the diffusive efficiency of the duct as indicated in the continuing climb of the cane curve into regions of higher bleed. State 4 was the operating point of the diffuser. This point is known as the *critical point* and serves as our reference point for discussions of the overall diffuser performance in terms of AATPR, distortion intensity, and general flow field characteristics.
5. In state 5 the terminal shock had been backpressured to (approximately) the upstream end of the porous bleed band.
6. State 6 is our sub-critical state. Here the terminal shock sat just downstream of the C-D nozzle.

Figure 11 compares the cane recovery curves of the L/D = 2.3, AR = 1.9 diffuser to the L/D = 2.7, AR = 1.6 model, both with a super-critical bleed of 5%. It is interesting to note that the recovery versus bleed behavior was nearly identical for both diffusers and that no noticeable recovery performance penalty was incurred for the more compact diffuser.

Baseline Results at the Critical Point

Figure 12 compares low and high-resolution engine face Pitot profiles of the L/D = 2.3, AR = 1.9 diffuser at the critical point. Again, the supercritical bleed was 5%. Notice how the low-resolution grid fails to capture the ramp wake pressure defect clearly visible in the high-resolution profile (at the 3 and 9 o'clock positions). What are well captured by the low-resolution grid, however, are the thick boundary layers at the 6 and 12 o'clock positions. As mentioned previously, in regard to the results obtained in the longer diffuser and illustrated in Figures 3 and 4, these thick boundary layers arose, in part, to a flow separation originating at the bypass cavity just upstream of the engine face. To see if that phenomenon was occurring in this instance, a surface oil flow visualization test was conducted on the compact diffuser operating at the critical point. Figure 13 shows the results, and clearly indicates a flow separation originating near the bypass cavity in a manner analogous to that described for the longer duct.

Figure 14 illustrates the radial profile of circumferential distortion intensity in the baseline duct. This distortion pattern shows a distinct two-lump feature attributable to characteristics of the engine face Pitot pressure profile. Near the hub, the distortion was dominated by the influence of the high momentum core flow (straddling the hub at top and bottom) and the ramp wake (left and right of the centerbody). These elements contributed to the first peak at $r/R \approx 0.4$. Near the cowl, the broad regions of low momentum fluid produced by the cavity-driven separation were responsible for driving the distortion even higher. The peak intensity of the second lump was about 8% where $r/R \approx 0.7$. The sharp "valley" of low distortion occurring between peaks results from the core region of high momentum fluid on either the top or bottom side of the centerbody.

Suppression of Cavity-Driven Flow Separation

The first flow control technique attempted was an application of vortex generators. The vortex generators used each shed a trailing longitudinal vortex into the developing boundary layer of the diffuser. The overall strategy was to combine these vortices into a convective pattern that countered the flow upwelling from the 6 and 12 o'clock positions of the bypass cavity. Figure 15 illustrates how this pattern was constructed. Figure 15 is a cross-section of the diffuser at the vortex generator mounting location. On the top cowl surface, six vortex generators were used to produce a strong down flow on the diffuser cowl centerline. An identical pattern of vortex generators produced a similar result on the bottom cowl surface.

The second technique used was an installation of the bypass cover plate. As mentioned previously, this plate covered over the portion of the bypass cavity where the convection induced by the vortex lift-off

spilled fluid into the core flow. The cover plate was inserted into the bypass cavity so there was no protrusion of its edges into the flow.

The third technique was to use the vortex generators and bypass cover plate together.

Figure 16 illustrates the results of surface oil flow visualization conducted in the vicinity of the bypass cavity for each of the three flow control techniques described above. These surface streamline patterns indicate that, in each case, the flow separation is removed. Figure 17 shows the corresponding engine face Pitot pressure contours at the critical point. All three techniques are seen to reduce the cowl boundary layer thickness. Total pressure recovery is greatest for use of the bypass cover plate alone. The increase in total pressure recovery over baseline is more than 2 percent, a significant improvement. The use of vortex generators was less effective in raising the total pressure recovery due to the device drag associated with each vortex generator in the flow field. The total penalty for vortex generator use is about 1 percent of the total pressure recovery, based on a comparison of the results for use of the cover plate alone, and cover plate with vortex generators. Figure 18 compares the radial profile of circumferential distortion intensity derived from the data plotted in Figure 17. We see that the first peak in distortion intensity (near the hub) and the sharp dip or valley, are drawn out to larger radius for all cases with flow control. This results from the relocation to larger radius of the high momentum core fluid. We also see that the second peak is substantially reduced in size. This reduction in the second peak is tied to the thinning of the cowl boundary layers and is also reflected in the reduction of the DC60 parameter. The greatest reduction in DC60 occurs for the test case using both vortex generators and bypass cover plate. The result is about 70 percent less than baseline. Like the increase in total pressure recovery, this is also a substantial performance improvement.

Summary

A facility was designed to test the bifurcated subsonic diffuser of a mixed compression inlet. Inflow and exit flow conditions were closely matched to those occurring in a full supersonic inlet. A terminal shock at the inflow region could be positioned over active bleed surfaces in the throat using a downstream backpressuring plug. The bifurcated subsonic diffuser tested had an L/D = 2.30 and an AIP-to-throat cross-sectional area ratio of 1.90. Flow separation was observed to occur in the baseline duct operating at the critical point (with the terminal shock at the diffuser geometric throat). This flow separation was traced to the bypass cavity feature where a vortex lift-off phenomenon was observed. An application of vortex generators and/or a partitioned bypass cover plate were found to remove this separation and improve the operating characteristics of the diffuser. The use of vortex generators and bypass cover plate together worked best for reducing the circumferential distortion intensity at the critical point, where a 70% drop in DC60 (relative to baseline) occurred. The use of the cover plate alone worked best for increasing the area-averaged total pressure recovery at the critical point, where an increase of 2% over baseline occurred. An important question still remains: Does the reduced bypass cavity entrance area adversely affect the required bypass flow capability for the “locked rotor” engine condition? The answer to this question will require the future testing of a full mixed compression inlet system equipped with the appropriate fast-response systems.

Reference

[1,2]Wasserbauer, J. F., Meleason, E. T. and Burstadt, P. L., “Experimental Investigation of the Performance of a Mach 2.7 Two-Dimensional Bifurcated Duct Inlet With 30 Percent Internal Contraction,” NASA TM–106728, Cleveland, Ohio, May 1996.

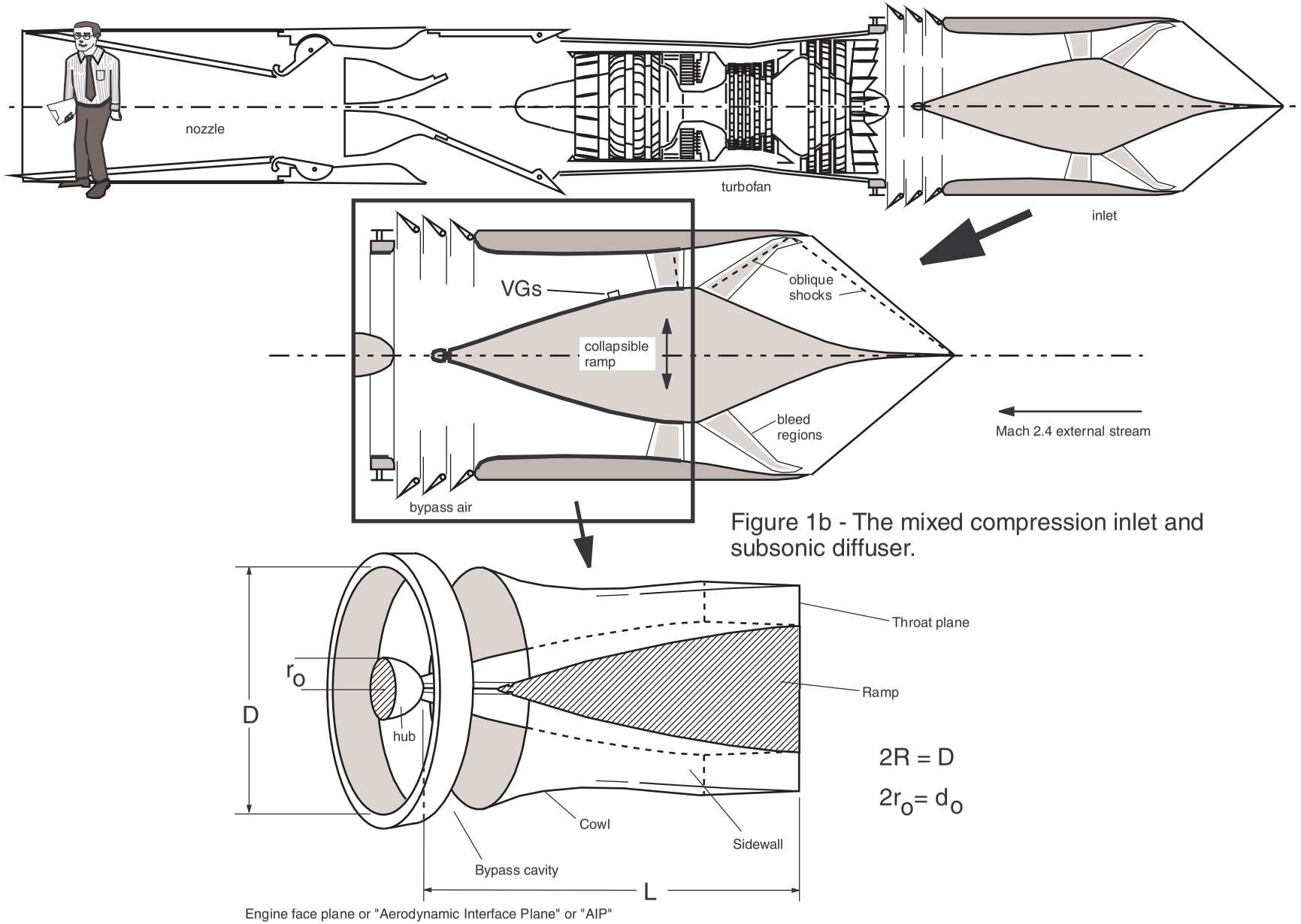

Figure 1b - The mixed compression inlet and subsonic diffuser.

Figure 1a - The HSR propulsion system.

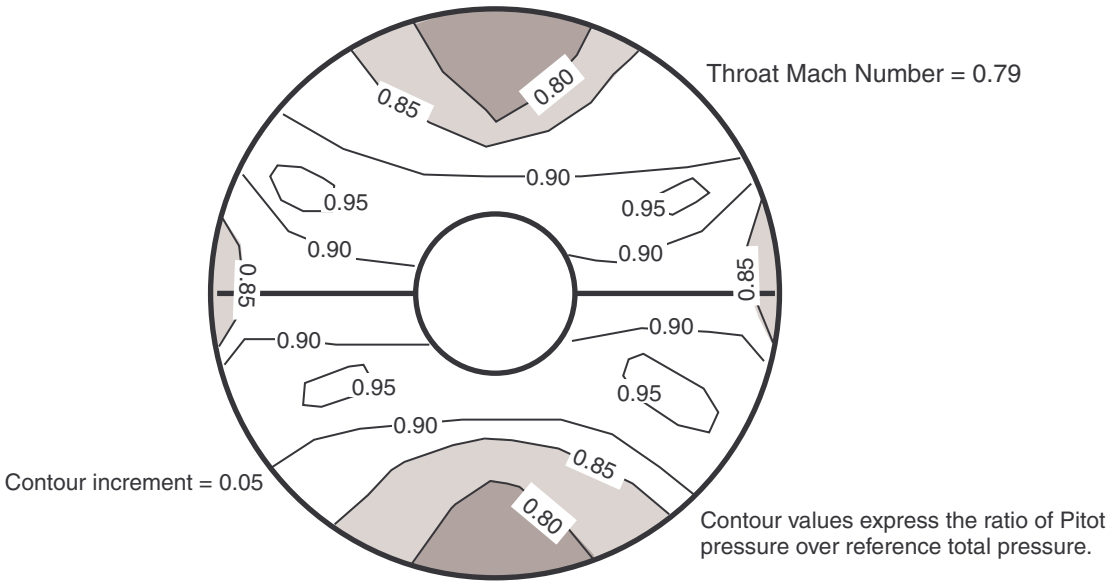

Figure 2 - Engine face Pitot pressure contour plot for a bifucated subsonic diffuser with L/D = 3.2.

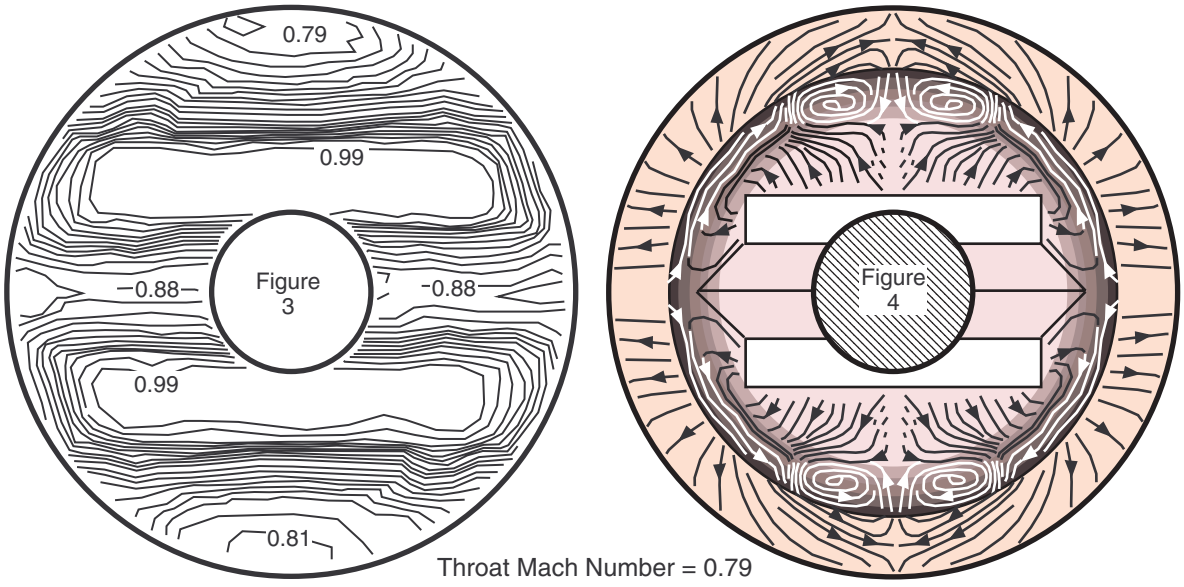

Figures 3 and 4 - High resolution Pitot pressure surveys at the engine face, and surface oil flow visualization reveal the effects of a cavity-driven vortical lift-off and flow separation in a bifurcated diffuser with L/D = 3.0. The dark band in Figure 4 represents the downstream facing portion of the bypass cavity. The lighter outer band in Figure 4 represents the cowl annulus surface (on which flow reattachment is seen to occur).

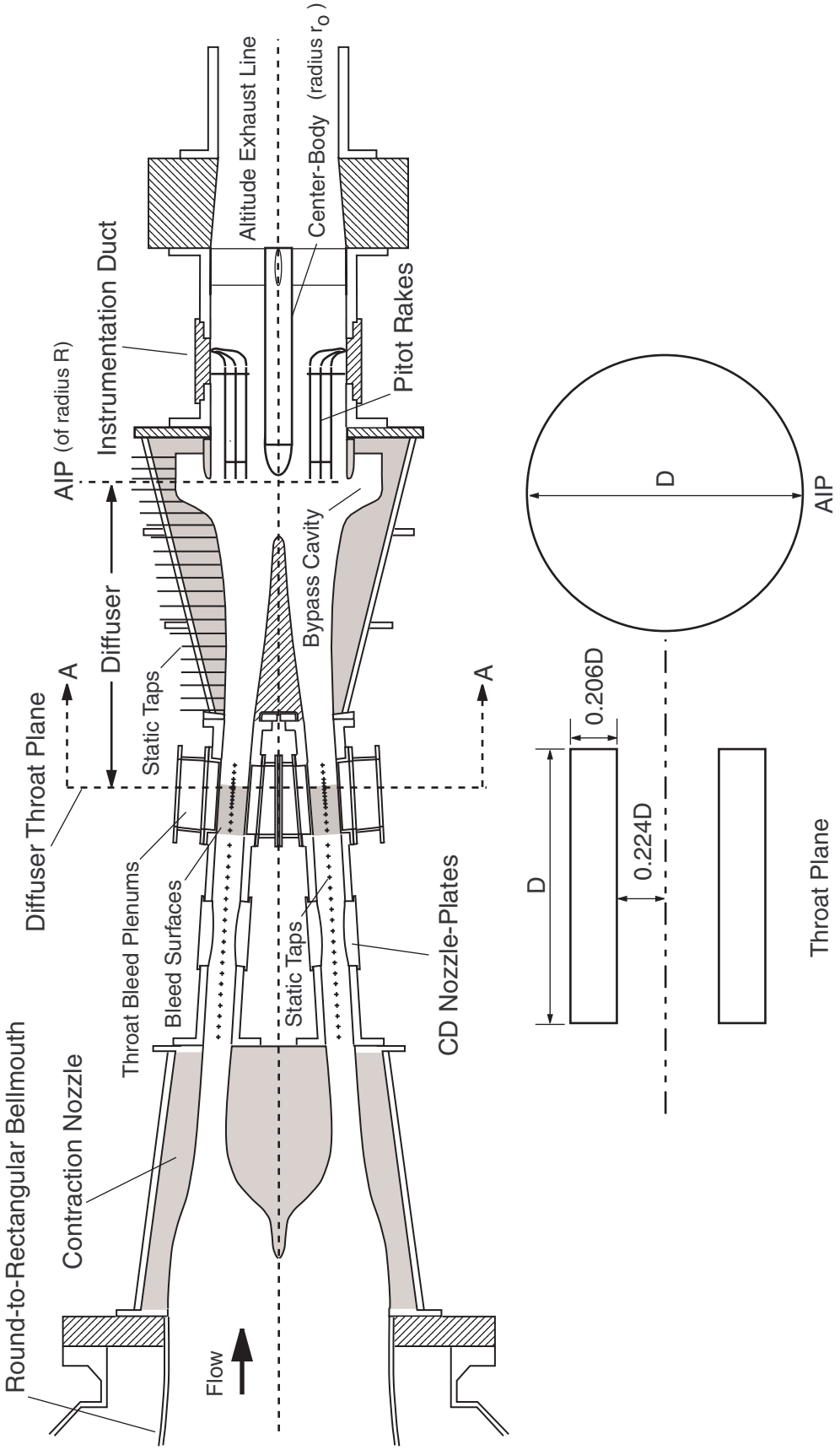

Figure 5 - The bifurcated subsonic diffuser test section.

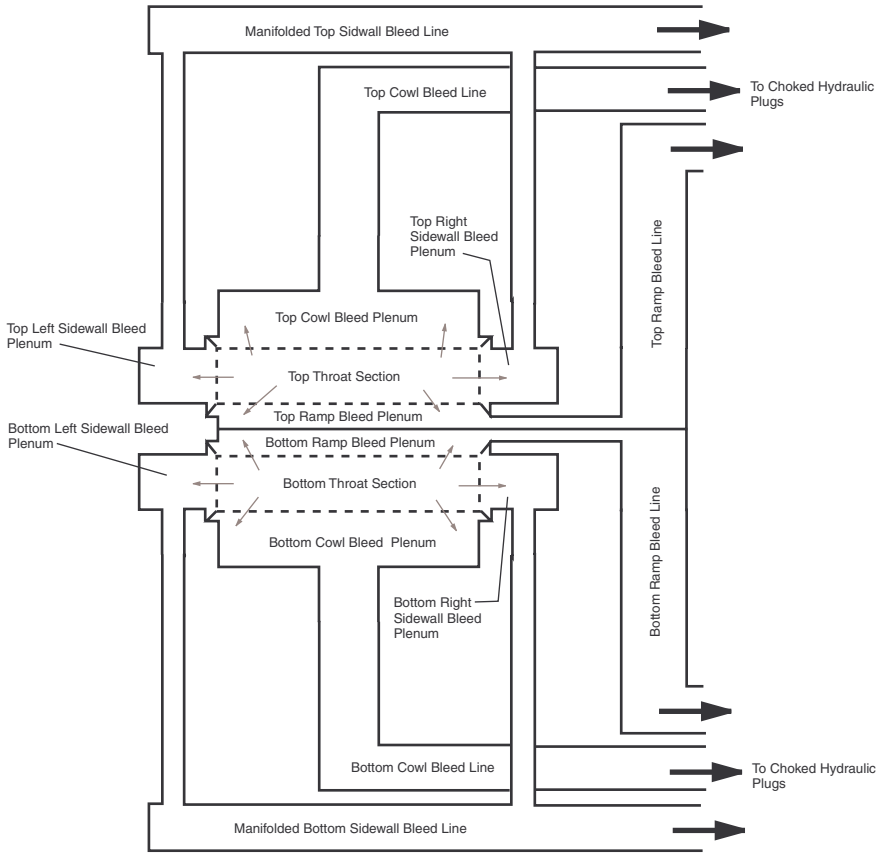

Figure 6 - Expanded Throat Cross-Section (A-A from Figure 5) Showing Wall Bleed Plenums and Bleed Lines.

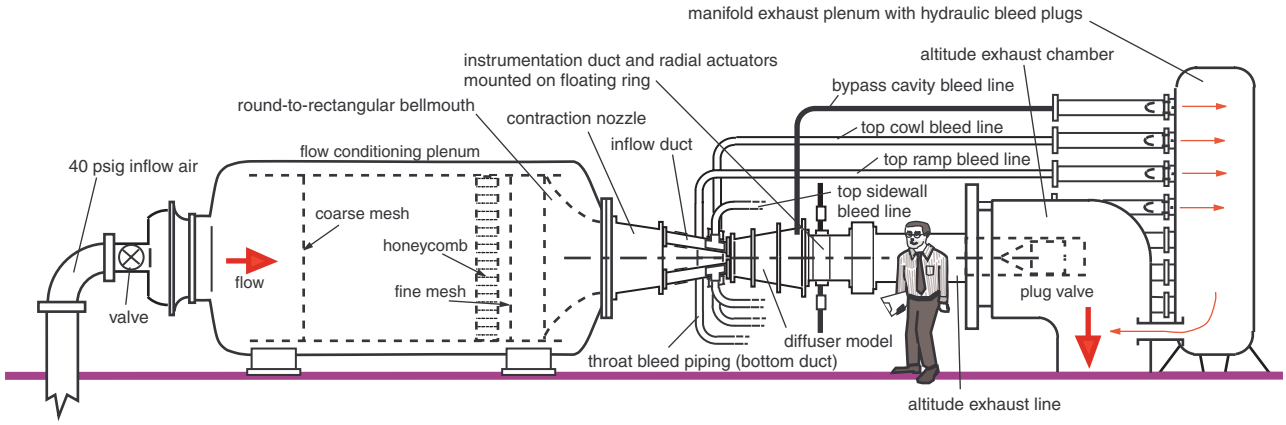

Figure 7 - The W1B Diffuser Test Facility

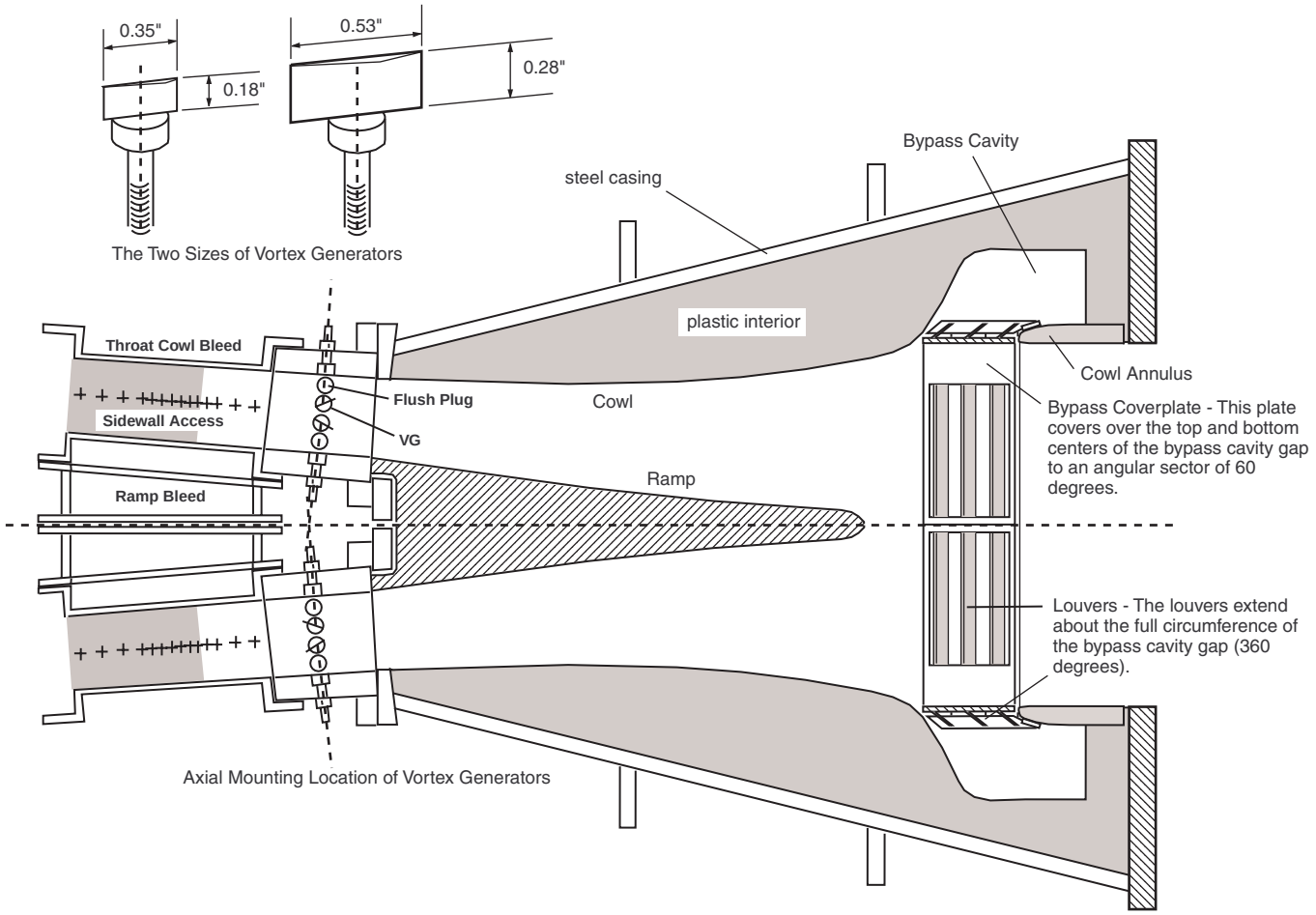

Figure 8 - The Flow Control Features of the Compact Diffuser Model

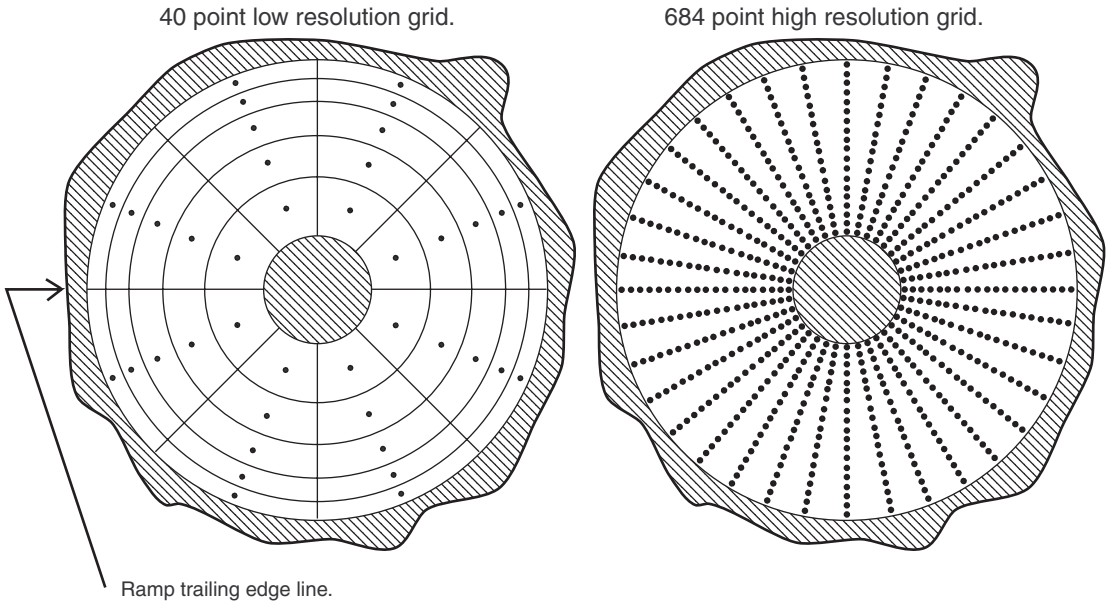

Figure 9 - Pitot pressure survey grids at the engine face plane.

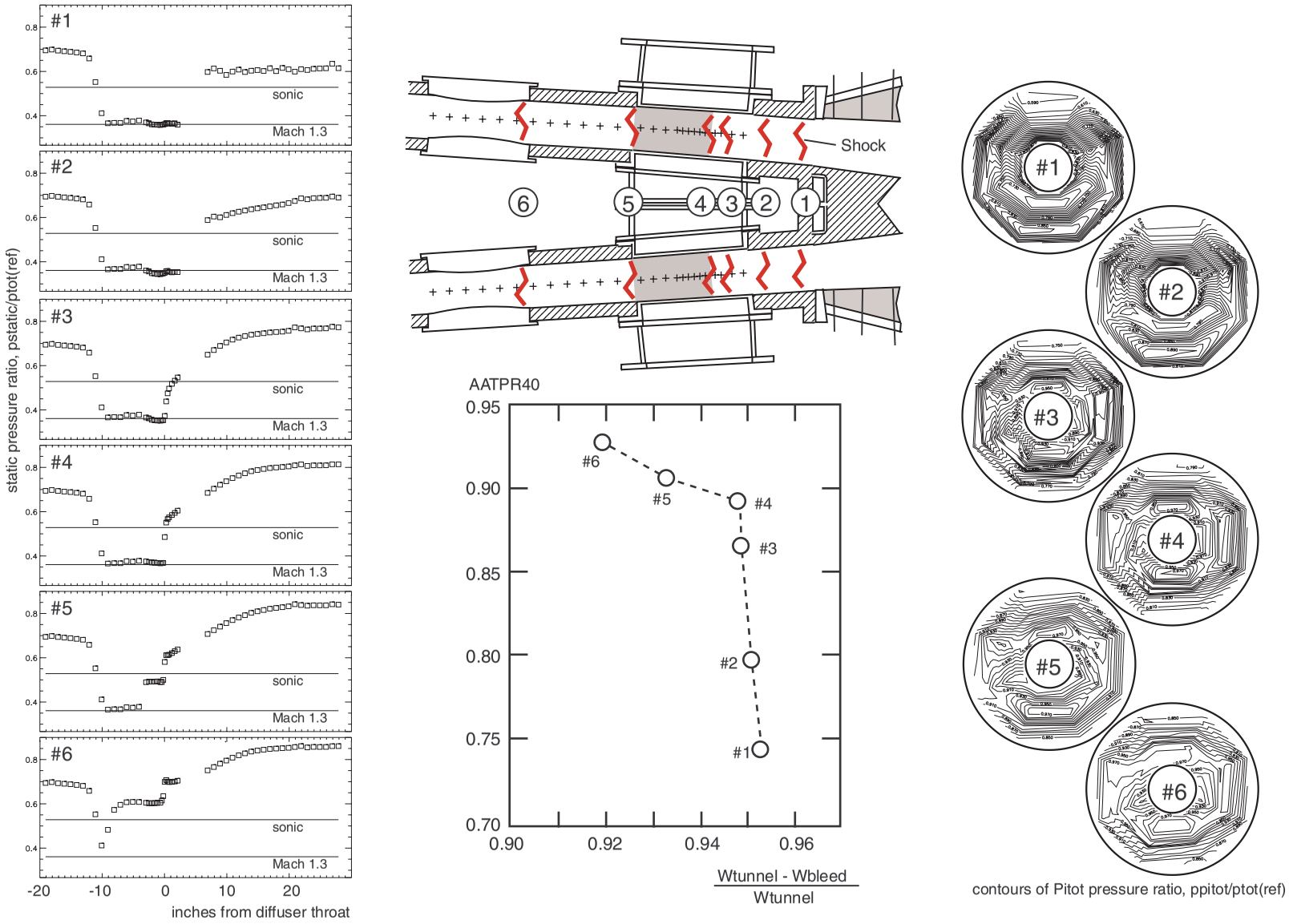

Figure 10 - Shock location versus bleed and recovery performance for the compact bifurcated diffuser.

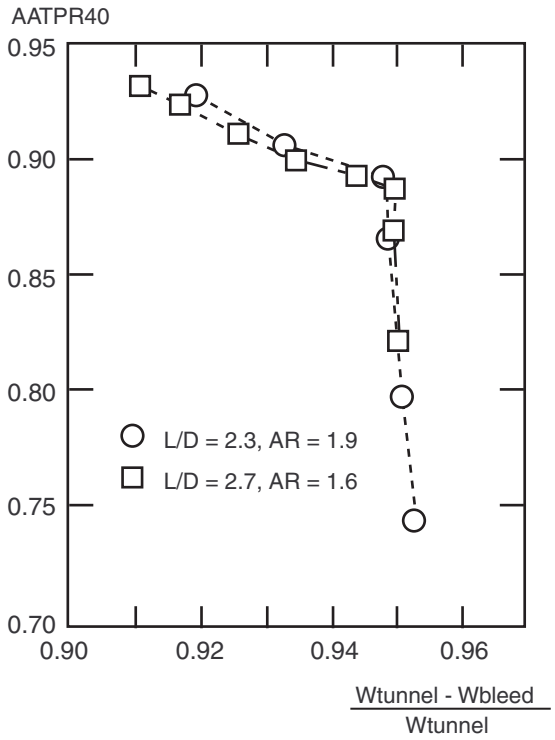

Figure 11 - The bleed versus recovery performance of the baseline diffusers.

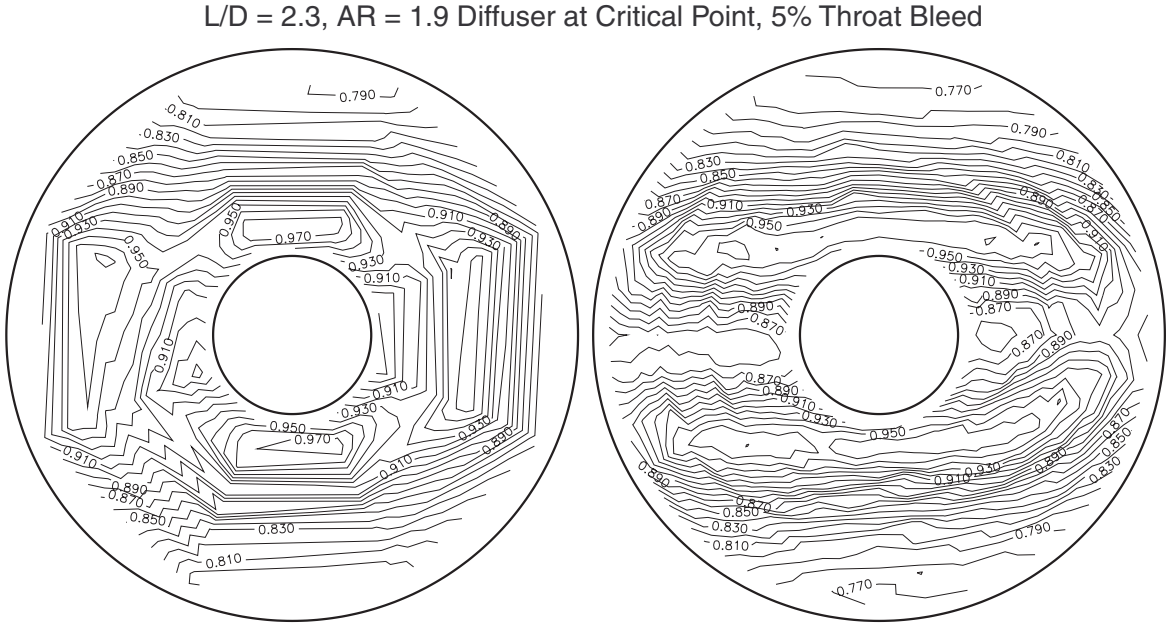

Figure 12 - A comparison of the low and high resolution Pitot pressure surveys of the baseline L/D = 2.3 diffuser

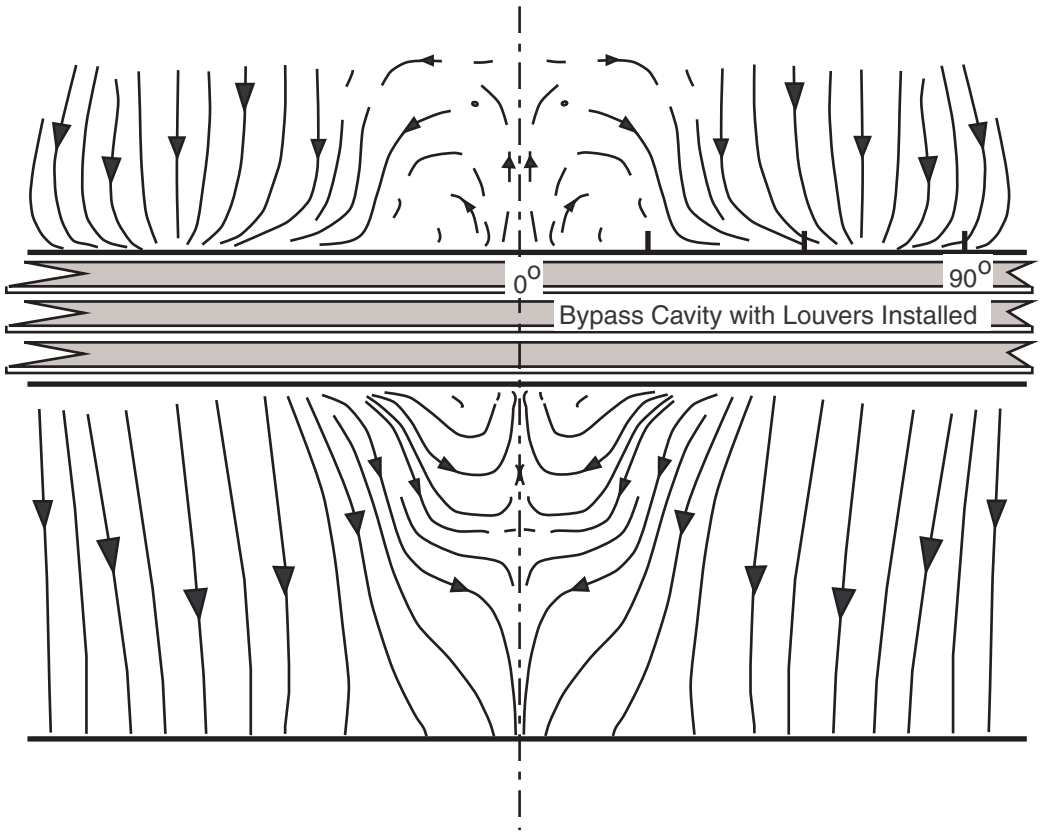

Figure 13 - Surface streamlines in the vicinity of the bypass cavity, derived from oil flows.

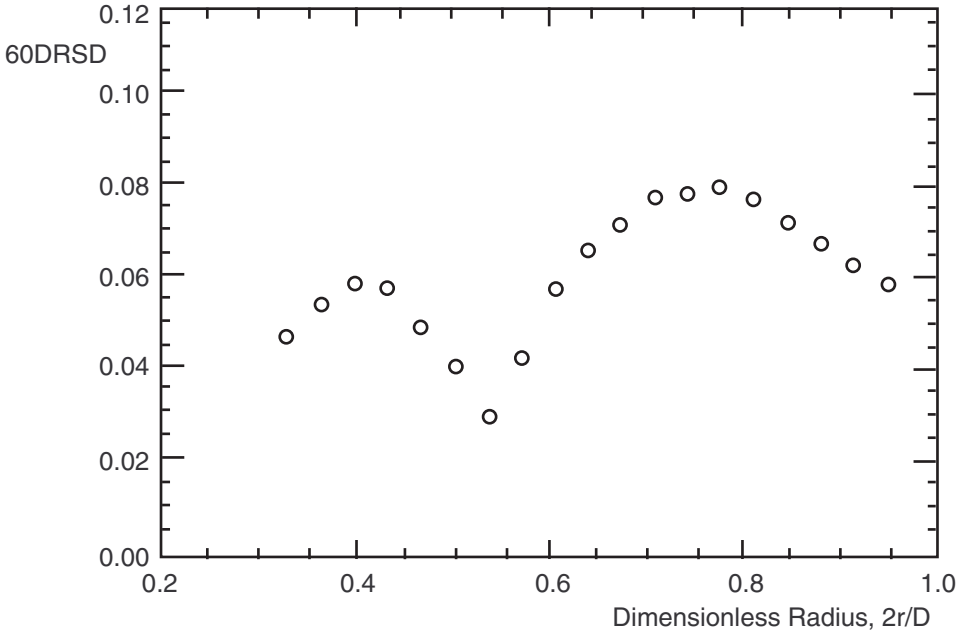

Figure 14 - Baseline distortion.

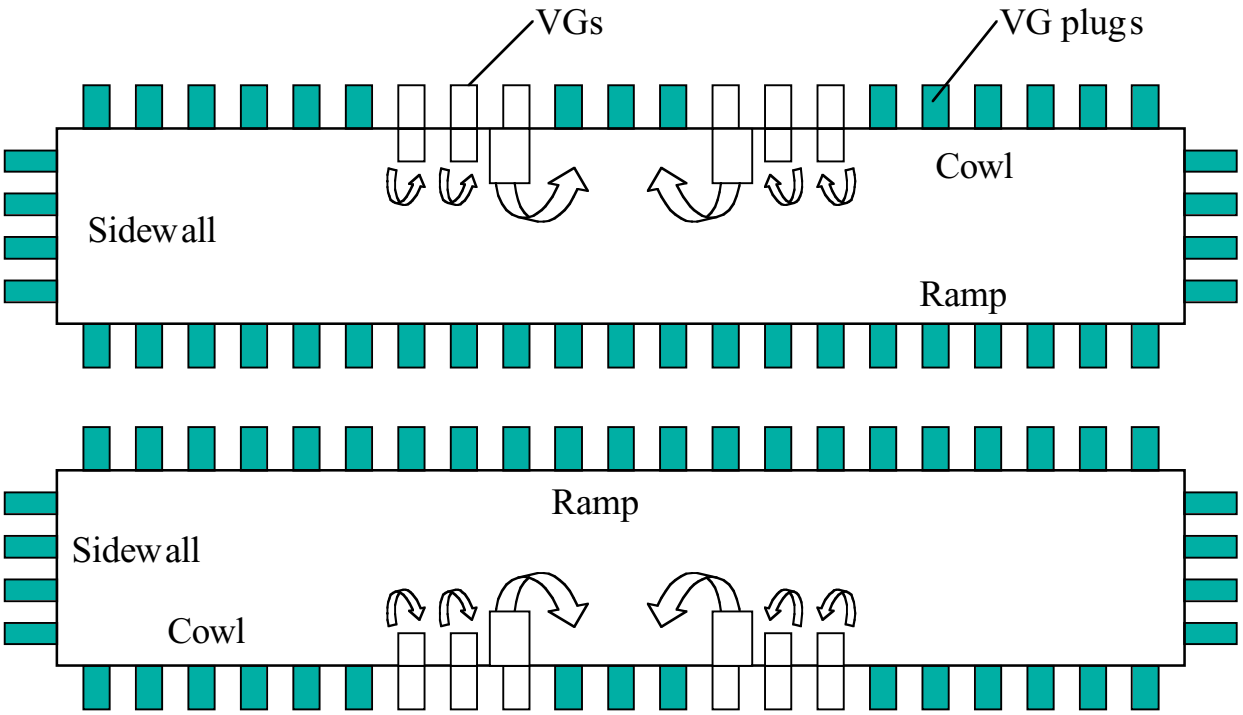

Figure 15 - Diffuser cross-section at the mounting location of the vortex generators. The 12 vortex generators used are set to produce a convective pattern which counters the upwelling induced by the downstream cavity-driven flow separation.

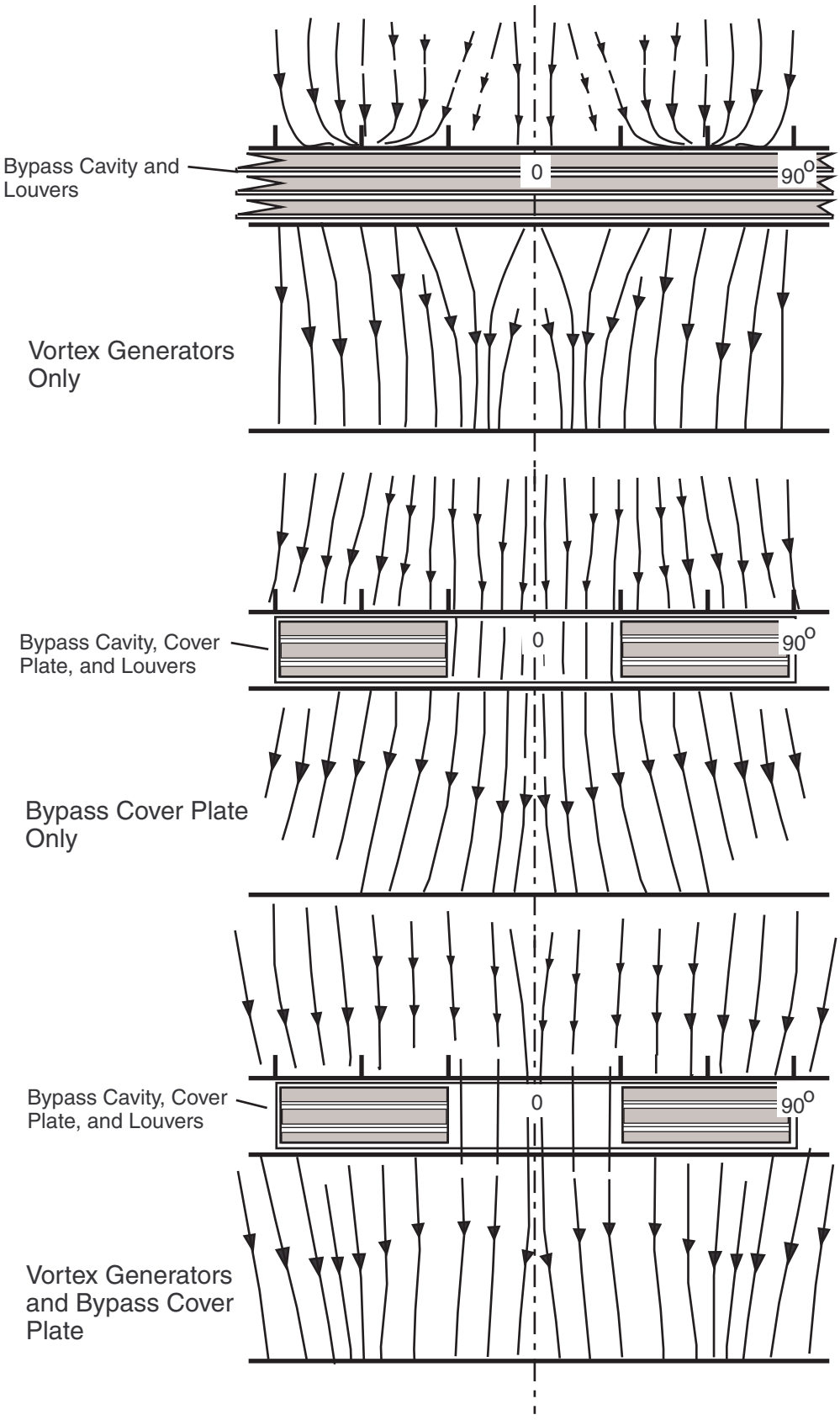

Figure 16 - Flow visualization results in the region of the bypass cavity for the diffuser operating at the critical point, for three types of flow control.

L/D = 2.3, AR = 1.9 Diffuser at Critical Point, 5% Throat Bleed

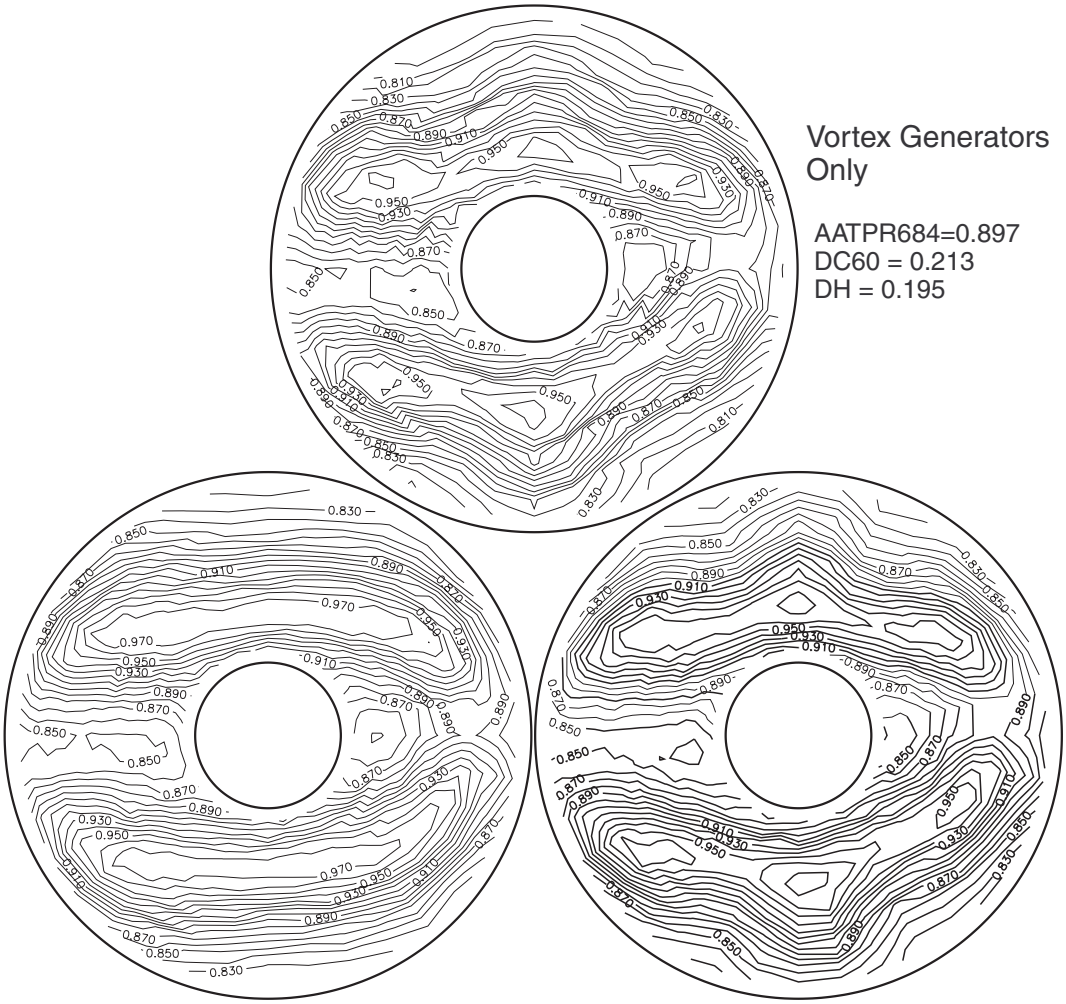

Vortex Generators Only

AATPR684=0.897
DC60 = 0.213
DH = 0.195

Bypass Coverplate Only

AATPR684 = 0.913
DC60 = 0.246
DH = 0.181

Vortex Generators and Bypass Coverplate

AATPR684 = 0.904
DC60 = 0.154
DH = 0.206

Figure 17 - High resolution Pitot surveys at the engine face for various flow configurations.

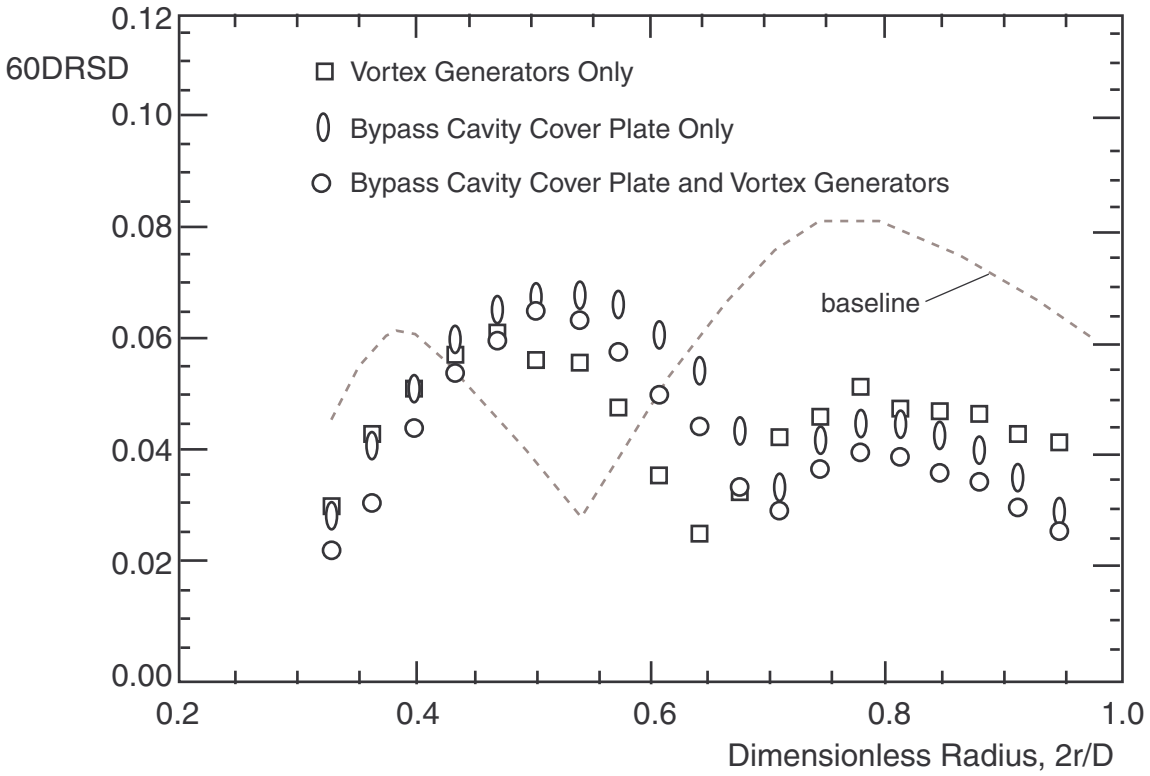

Figure 18 - Sixty degree ring sector distortion results for the diffuser operating at the critical point, for three types of flow control.

REPORT DOCUMENTATION PAGE

Form Approved
OMB No. 0704-0188

1. AGENCY USE ONLY (*Leave blank*)	2. REPORT DATE	3. REPORT TYPE AND DATES COVERED
	September 2000	Final Contractor Report

4. TITLE AND SUBTITLE

Suppression of Cavity-Driven Flow Separation in a Simulated Mixed Compression Inlet

5. FUNDING NUMBERS

WU–523–90–43–00
NAS3–99138

6. AUTHOR(S)

Bruce J. Wendt

7. PERFORMING ORGANIZATION NAME(S) AND ADDRESS(ES)

Modern Technologies Corporation
7530 Lucerne Drive
Islander Two, Suite 206
Middleburg Heights, Ohio 44130

8. PERFORMING ORGANIZATION REPORT NUMBER

E–12456

9. SPONSORING/MONITORING AGENCY NAME(S) AND ADDRESS(ES)

National Aeronautics and Space Administration
Washington, DC 20546–0001

10. SPONSORING/MONITORING AGENCY REPORT NUMBER

NASA CR—2000-210460

11. SUPPLEMENTARY NOTES

Project Manager, Tom Biesiadny, Turbomachinery and Propulsion Systems Division, NASA Glenn Research Center, organization code 5850, (216) 433–3967.

12a. DISTRIBUTION/AVAILABILITY STATEMENT

Unclassified - Unlimited
Subject Categories: 07, 02 and 01 Distribution: Nonstandard

This publication is available from the NASA Center for AeroSpace Information, (301) 621–0390.

12b. DISTRIBUTION CODE

13. ABSTRACT ***(Maximum 200 words)***

A test facility designed to simulate a bifurcated subsonic diffuser operating within a mixed compression inlet is described. The subsonic diffuser in this facility modeled a bypass cavity feature often used in mixed compression inlets for engine flow matching and normal shock control. A bypass cavity-driven flow separation was seen to occur in the subsonic diffuser without applied flow control. Flow control in the form of vortex generators and/or a partitioned bypass cavity cover plate were used to eliminate this flow separation, providing a 2 percent increase in area-averaged total pressure recovery, and a 70 percent reduction in circumferential distortion intensity.

14. SUBJECT TERMS

Supersonic inlet; Vortex generators; Separated flow

15. NUMBER OF PAGES

24

16. PRICE CODE

A03

17. SECURITY CLASSIFICATION OF REPORT	18. SECURITY CLASSIFICATION OF THIS PAGE	19. SECURITY CLASSIFICATION OF ABSTRACT	20. LIMITATION OF ABSTRACT
Unclassified	Unclassified	Unclassified	